International Symposium of Research Students on Material Science and Engineering
December 20-22, 2004, Chennai, India
Department of Metallurgical and Materials Engineering, Indian Institute of Technology Madras

HOT WORKING AND MODELING OF THE RESULTING MICROSTRUCTURE OF D-9 STAINLESS STEEL USING ARTIFICIAL NEURAL NETWORKS

Sumantra Mandal, P.V. Sivaprasad and R.K. Dube*
Metallurgy and Materials Group Indira Gandhi Centre for Atomic Research
Kalpakkam – 603 102, Tamilnadu
** Department of Metallurgical Engineering Indian Institute of Technology, Kanpur*

ABSTRACT

The paper discusses the kinetics and mechanism of dynamic recrystallization (DRX) behaviour in a 15Cr-15Ni-2.3Mo-Ti modified austenitic stainless steel and modelling the resulting microstructure using artificial neural networks (ANN). Drop hammer forging and hydraulic press forging operations have been carried out in the temperature range 950°C-1150°C to various strain levels in the range 0.1 to 0.5. Kinetics of the dynamic recrystallization (DRX) was studied with the help of hardness measurements and it has been shown that it obeys the modified JMAK (Johnson-Mehl-Avrami-Kolmogorov) model with Avrami exponent falling in the range 1.07 to 1.41. Optical metallography revealed that new DRX grains are generated along prior grain boundaries by 'bulging mechanism'. From electron back scattered diffraction (EBSD) study, it is proposed that twins may play an important role for the expansion of DRX grains through the deformed matrix. It is found that γ fibre is strong while α fibre is weak in the recrystallized matrix. The paper discusses modelling the microstructure during DRX in order to replace the conventional trial and error technique to manipulate the product microstructure, which was based on developing multilayer perceptron based artificial neural network (ANN) models.

1. INTRODUCTION

Alloy D-9 (15Cr-15Ni-2.3Mo-Ti modified austenitic stainless steel) is proposed to be used for fuel clad and fuel sub-assembly wrapper in Prototype Fast Breeder Reactor (PFBR) of Indian nuclear programme owing to its high resistance to void swelling and irradiation embrittlement. This material has to be subjected to various thermo-mechanical processes prior to the fabrication of the components. During processing, the material undergoes shape change as well as changes to the microstructure that depends on the process history. While the tooling decides the shape and size of the product, the properties of the product depend on the thermomechanical history the product has seen. Hence to achieve the required properties and microstructure, a careful selection and monitoring of processing parameters like strain, strain rate and temperature during thermomechanical processes is essential. Sivaprasad et al [1,2] have identified the optimum processing parameters for hot working of the alloy based on processing maps and confirmed the results with industrial validation tests. The aim of the present investigation is to understand the kinetics and mechanism of deformation processes for the in-core material. Another important consideration of the present study is to model the microstructure during hot working operation of D-9 material. The modeling of microstructure during high temperature metal working operation not only saves the energy and manpower, but also the time that ultimately enhanses the productivity.

2. EXPERIMENTAL

The alloy D-9 used in this present investigation was supplied by M/s. MIDHANI, Hyderabad, India, in mill annealed condition as 30-mm diameter rods. Chemical composition of the alloy is given in Table 1. The cast ingots were hot forged and hot rolled to 30-mm diameter rounds. Cold swaging operation was performed in order to reduce the diameter of the rod to 20 mm. The cold swaged rod was then annealed in a vacuum furnace at 1050°C for one hour in order to eliminate the effect of work hardening as well as to obtain complete recrystallized structure. The average grain size was 200 μm. From this homogenized rod, 30-mm height and 20 mm diameter compression specimens for forging operation were machined.

2.1. drop hammer forging operation

Hammer forging operations were carried out with a 250 kg pneumatic hammer in a single blow in the temperature region 950°C –1150°C in steps of 50°C. The mean strain rate of the forge hammer is about 100 s^{-1}, which has been measured using high-speed photography. Thickness strains of 10, 20, 30, 40 and 50% were imparted at each temperature in order to study the effect of strain on recrystallisation behaviour. The specified amount of strain in each sample was achieved in a single step. As soon as the operation was finished, the deformed specimen was water quenched with in 2-3 s in order to freeze the deformed microstructure.

2.2. hydraulic press forging operation

Hydraulic press-forging tests were performed on a 250-ton triple-action hydraulic press. The operations were carried out in the temperature region 950°C –1100°C in steps of 50°C. Similar to hammer forging tests, thickness strains of 10, 20, 30, 40 and 50% were imparted at each temperature for the generation of different microstructural states in order to pursue the microstructure evolution during DRX. The calculated mean strain rate during hydraulic press was equal to ≈ 0.20 s^{-1}.

2.3. Metallography and Microhardness measurements

The hot worked samples were cut along the longitudinal direction and one half of the sample was taken to prepare metallographic specimens. Metallographic specimens were polished and etched in 10% ammonium persulphate [$(NH_4)_2S_2O_8$] solution. The microstructures were examined optically in the maximum deformation zone of the samples and grain sizes were measured employing linear intercept method. Hardness measurements were made by Microhardness tester [HMV-2000 SHIMADZV] using 200-gram load. The measurements were taken on the maximum deformation zone of the sample. Fraction of recrystallization (%DRX) at different working conditions was calculated by employing the following equation:

$$\%DRX = \frac{H_{CW(x)} - H_{HW(x)}}{H_{CW(x)} - H_{SA}}$$

where $H_{CW(X)}$ denotes the hardness of the cold worked specimen at a strain level of x percent, $H_{HW(X)}$ is the hardness of the hot worked sample at same strain in a particular working temperature at which fraction of recrystallization is calculated, and H_{SA} denotes the hardness of solution annealed sample.

3. RESULTS AND DISCUSSION

The Johnson-Mehl, Avarami, Kolmogorov (JMAK) model has been extensively used to describe the recrystallization behaviour [3]. This model could be expressed mathematically by the Eq. (1) as follows:

$$X_V = 1 - \exp(-kt^n) \quad \ldots\ldots\ldots\ldots\ldots\ldots (1)$$

where X_V, recrystallization fraction at any annealing time t; k, constant; n, JMAK or Avrami exponent. This JMAK model has been used for static recrystallization where annealing time t is available. However, in the present case of hammer forging, the whole operation finishes in a fraction of second. So time t could not be accurately measured with present experimental facilities. Therefore this model in the present form could not be applied to investigate the kinetics of DRX. In the present study, some modification of JMAK model has been carried out in order to investigate the kinetics of DRX. The t term was replaced by ε, where ε is true strain. The modified JMAK model can be expressed by Eq. (2) as follows:

$$X_V = 1 - \exp(-k\varepsilon^n) \quad \ldots\ldots\ldots\ldots\ldots\ldots (2)$$

According to this modified model, if X_v vs. ε is plotted, it should yield a sigmoidal curve. In Fig. 1, the plot of X_v vs. ε for forge hammer operation has been shown.

From Fig. 1, it can be observed that the curves are sigmoidal in nature. At high temperature the curve is steeper compare to that of low temperature. This is because at high temperature, available thermal activation energy is more, which helps the process to be completed. The results for hydraulic press forging were also sigmoidal in nature.

According to the modified JMAK model, a plot of $ln(-ln(1- X_v))$ vs. $ln(\varepsilon)$ should yield a straight line whose slope will be equal to Avrami exponent n. Such relationship was plotted for hammer forged samples and is shown in Fig. 2. From these figures one can see that the plots are straight line in nature. So it can be corroborated that whatever modification of JMAK model have been done is perfectly matching with the experimental results. The values of Avrami exponent in different hot-working operations are tabulated in Table 2.

From the Table 2, it is evident that the value of Avrami exponent varies between 1.07 to 1.41. It has been observed from the present study that after hot working in the temperature range 950°C-1150°C, the product microstructure always consisted of finer grain size as compare to that of starting one. Such a behaviour can be attributed to the mechanism of growth controlled DRX in this alloy. In this mechanism, a large number of growing nuclei are formed and these growing nuclei mutually inhibit grain boundary mobility and restrict the grain growth. As a result, the product microstructure always leads to grain refinement as observed in the conditions considered in the present study. This type of DRX is also known as single peak dynamic recrystallization [4]. The low value of Avrami exponent obtained from the present study also conforms this behaviour. It is reported in the literature that low values of Avrami exponent leads to the nucleation of new strain free grains taking place in the interfacial area of grain and twin boundaries [5]. In the present study, metallographic observations (Fig. 3) support similar kind of behaviour reported for low Avarami exponent. So from the present study, it can be concluded that alloy D-9 shows growth controlled DRX in which nucleation of new DRX grains take place in the interfacial area of grain and twin boundaries.

3.1. mechanism of drx

Metallographic study shows that initiation of DRX takes place on the parent grain boundary by 'bulging mechanism'. At low temperature and low strain, the grain boundaries became serrated in nature which is the precursor stage of DRX (Fig. 3a). In Fig. 3b some small new dynamically recrystallized grains can be observed at grain boundaries and especially at triple junctions. With increasing temperature, many DRX grain appears in the deformed matrix and incomplete necklace structures developed (Fig. 3c and 3d).

The 'bulging mechanism' is able to describe as to how the first recrystallized grains and, correspondingly, the first layer of new grains around the prior grains (necklace structure) forms. But there is an almost complete lack of knowledge on the principle, which underlines the expansion of the necklace structure along the deformed volume. When in the course of DRX the pre-existing grain boundaries are entirely covered with new grains (site saturation), bulging would have to proceed from the small-recrystallized grains, which requires a very high boundary curvature. This makes further nucleation by bulging unlikely, because the very high driving force is necessary to offset the high surface tension of the bulge is not available in hot deformed microstructures [6]. So there is some other active mechanism which plays a crucial role for the expansion of the DRX grain through the deformed matrix.

The crucial step for nucleation of DRX in a subgrain structure is the generation of a mobile grain boundary. For small angle grain boundaries, the mobility increases with growing misorientation, but a rotation of 10 – 15° is commonly assumed to be necessary for nucleation to be occurred. To elucidate the role of subgrain near the grain boundaries with respect to expansion of DRX grain through the deformed matrix, electron back scattered diffraction (EBSD) study have been carried out. The misorientation distribution plot obtained from the EBSD study has been shown in Fig. 4. The plot reveals a frequency maximum at about 3° and a spread to higher angle. Misorientation in excess of 10° were only occasionally formed. It should be noted that, large angle misorientations were observed even though with a low frequency. These large misorientations were associated with twin boundaries and higher order twin orientations possibly rotated owing to progressive deformation [7]. So, from the present study, it has been seen that misorientation angle larger than 10° was rarely observed. Thus, continuous subgrain rotation near the large angle boundaries could not be attributed for the expansion of DRX grain through the deformed matrix.

In contrast, the frequency of large angle misorientation especially twin relations inside the subgrain structure is relatively high compared to the frequency of misorientation angles between 10 –15°. This large angle misorientation could not be accounted to continuous subgrain rotation as progressive subgrain rotation produce larger misorientation angles to its entire environment, which was not found in the current study. Rather, these large misorientations could be attributed to twining processes in the substructure in analogy to the behavior of single crystal [8]. So, it seems twining play an important role during the expansion of DRX grain through the deformed matrix. However, the exact mechanism of twin formation inside the subgrain structure could not be envisaged from the present study. In single crystals, twins are generated by interactions of dislocations inside the subgrain boundary or dissociations of cluster of dislocations [8]. Since, alloy D-9 is a polycrystalline material, the above mechanism of twin formations may not work and needs to be confirmed.

3.2 Ann Modeling

ANNs are mathematical models constituted by several neurons, arranged in different layers (input, hidden and output), interconnected through a complex network [9]. It has an excellent

ability to learn and to generalize (interpolate) the complicated relationship between input and output variables. In the present modeling work, a multilayer perceptron based ANN has been used since multi-layer network has a greater representational power for dealing with highly non-linear, strongly coupled, multi-variable system. Feed-forward network with a back propagation (BP) optimization scheme was used to train the network. During the training session of the network, a pair of patterns is presented (x_j, y_j), where x_j is the input pattern and y_j is the target or desired pattern. The x_j pattern causes output responses at each neuron in each layer and, hence, an actual output $y_j^{'}$ at the output layer. At the output layer, the difference between actual and target outputs yields an error signal. This error signal is depends on the values of the weights of the neuron in each layer. The error is minimized, and during this process new values for the weights are obtained. The speed and the accuracy of the learning process that is, the process of updating the weights also depend on a factor known as the learning rate [10].

To properly train and test the neural networks, experimental data is normalized in the range between 0 and 1. The convergence criterion for the developed networks is determined by the average root-mean-square (R.M.S) error E_{RMS} between the desired output value y_j and predicted output value $y_j^{'}$, i.e.:

$$E_{RMS} = \frac{1}{p}\sum_{i=1}^{p}\sqrt{\frac{1}{n}\sum_{j=1}^{n}(y_{ji} - y_{ji}^{/})^2}$$

where p is the number of training or testing data and n is the number of variable in the output vector [11].

3.2.1 Ann Model

In this model temperature, strain and strain rate have been fed as input while both %DRX and grain size have been obtained as output. So, the numbers of input neurons were 3 while numbers of output neurons were 2. The performance of the network at different hidden node has been analysed and found that the minimum RMS test error is obtained when number of hidden nodes are 6. The RMS training and test error of this model is found to be 0.06 and 0.1 respectively. Figure 5 shows the graphical comparison between experimental and predicted test data. In this plot, DRX is the experimental data and MLP_DRX is the predicted data obtained from the developed model. The correlation coefficient (R) between experimental and predicted data has been obtained by linear fitting of the experimental vs. predicted data as 0.89 for grain size data and 1.002 for DRX data. This reflects the excellent predictive capability of the present constructed model.

4. CONCLUSIONS

1. The experimental recrystallization kinetics measurements of Alloy D-9 have been found to agree with the modified model, represented by $X_v = 1\text{-}exp(-k\varepsilon^n)$. It suggests that modification carried out in JMAK model conforms to the experimental results.
2. The value of Avrami exponent calculated in the present study varies between 1.07–1.41. Metallographic observations showed that the nucleation of new strain free grains during DRX in alloy D-9 takes place at the grain and twin boundary surface. This correlates well with the reported literature value of Avrami exponent and the corresponding nucleation mechanism of DRX.
3. The microstructural study shows that during DRX, formation of new grain takes place on the parent grain boundary by ‘bulging mechanism’. Continuous sub-grain rotation is not found in the recrystallized D-9 based on the EBSD analysis.

4. Large misorientation (>55°) observed in the EBSD patterns is attributed to formation of twins during DRX. Twining seems to play an important role during the nucleation of DRX. However, their origin and exact role is poorly understood and needs further extensive study.
5. This study has shown the capability of an ANN-based system to predict the grain size and therefore microstructure of alloy D-9 during thermomechanical processing.

5. REFERENCES

1. P.V. Sivaprasad, S.L. Mannan, Y.V.R.K. Prasad and R.C. Chaturvedi, Identification of processing parameters for a 15Cr-15Ni-2.2Mo-0.3Ti austenitic stainless steel – A study using processing maps, Mater. Sci. Technol., 2002, Vol. 17, p. 545.
2. P.V. Sivaprasad, S.Venugopal, S. Venugopal, V.M. Muthu, M. Vasudevan, S.L. Mannan, Y.V.R.K. Prasad and R.C. Chaturvedi, Validation of processing maps for a 15Cr-15Ni-2.2Mo-0.3Ti austenitic stainless steel using hot forging and rolling tests, J. Mater. Proc. Technol., 2003, Vol.132, Iss.1-3 , p.262.
3. Weiping Ye, Rene Le Gall, Gay Saindrenan, Materials Science and Engineering A, 2002, 332, 41-46.
4. M.E1 Wahabi, J.M. Cabrera, J.M. Prado, Materials Science and Engineering A, 2003, 343, 116-225.
5. Sakai and J.J. Jonas, Acta Metallurgica, 1984, 32, (2), p. 189.
6. D. Ponge and G. Gottstein, Acta Materialia, 1998, 46, (1), p. 69.
7. E. Brunger, X. Wang and G. Gottstein, Scripta Materialia, 1998, 38, (12), p. 1843.
8. P. Karduck, G. Gottstein and H. Mecking, Acta Materialia, 1983, 31, p. 1525.
9. S. Calcaterra, G. Campana and L. Tomesani, Prediction of mechanical properties in spheroidal cast iron by neural networks, Journal of Materials Processing Technology, Vol. 104, 2000, p. 74.
10. S.V. Kartalopoulos, Understanding neural networks and fuzzy logic: Basic concepts and application, Prentice Hall of India, New Delhi, 2002, p. 76.
11. S.C. Juang, Y.S. Tarng and H.R. Lii, A comparison between the back-propagation and counter-propagation networks in the modeling of the TIG welding process, Journal of Materials Processing Technology, Vol. 75, 1998, p. 58.

TABLES

Table 1: Chemical composition of Alloy D-9

C	Mn	Si	S	P	Cr	Ni	Mo	Ti	B	Co	N
0.05	1.509	0.5	0.002	0.01	15.05	15.06	2.25	0.3	0.001	0.01	0.006

Table 2 Avrami exponent 'n' for hammer forged and hydraulic press forged products at different temperatures.

Hot working Temperature (°C)	Avrami exponent value (n)	
	Forge Hammer	Hydraulic Press
950	1.29	1.24
1000	1.31	1.13
1050	1.39	1.22
1100	1.40	1.07
1150	1.41	–

FIGURES

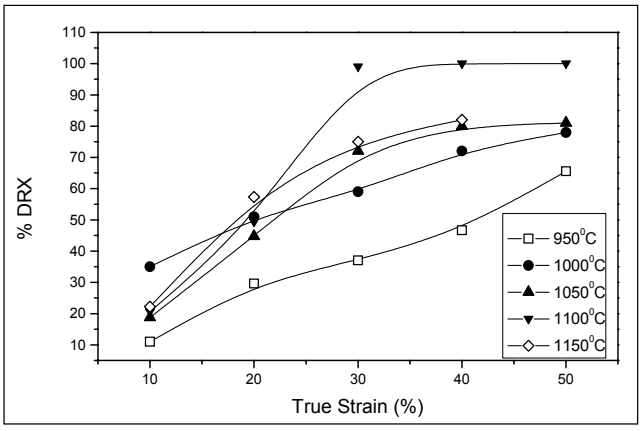

Figure 1: Effect of true strain on recrystallization kinetics at various temperatures during drop hammer forging operation

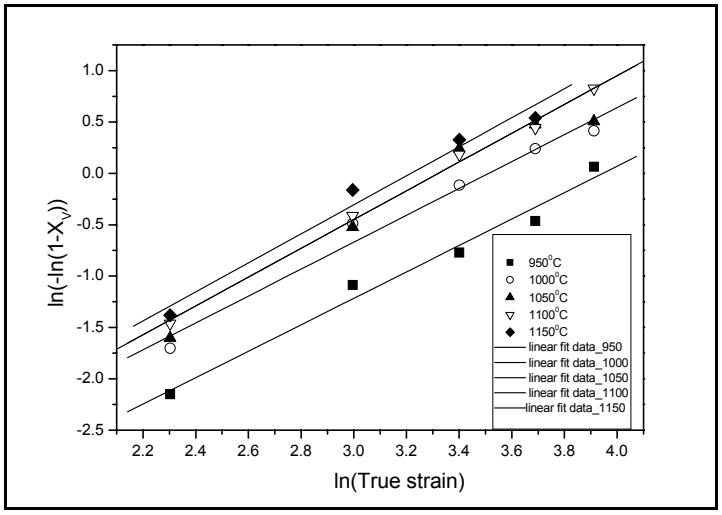

Figure 2: Modified JMAK plot of recrystallization kinetics at various temperatures in drop hammer forging operation

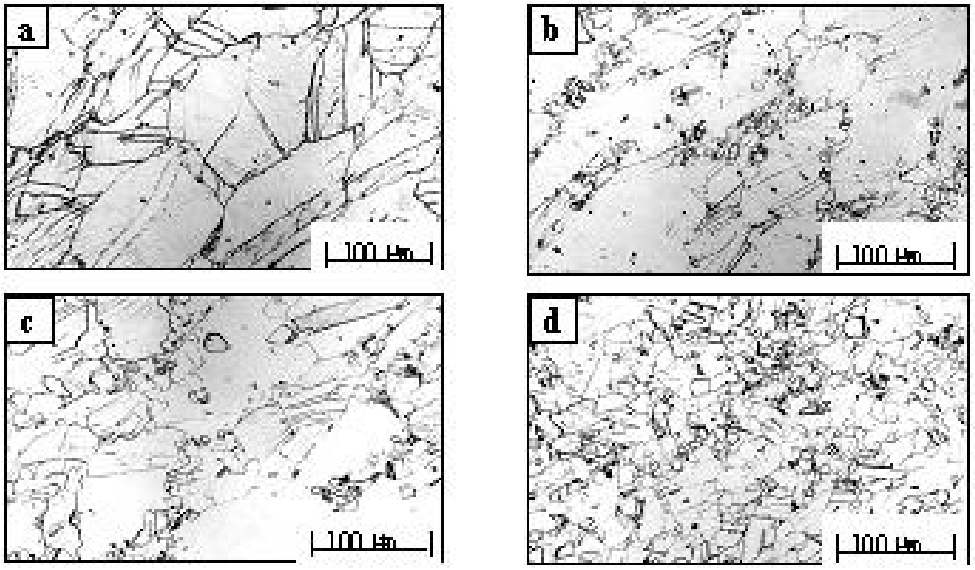

Figure 3: Microstructure evolution during hot working of alloys D-9
(a) Hydraulic press: T = 950°C, ε = 30% (b) Forge hammer: T = 950°C, ε = 28% (c) Forge hammer: T=1000°C, ε=28% (d) (d) Forge hammer: T=1150°C, ε=46%

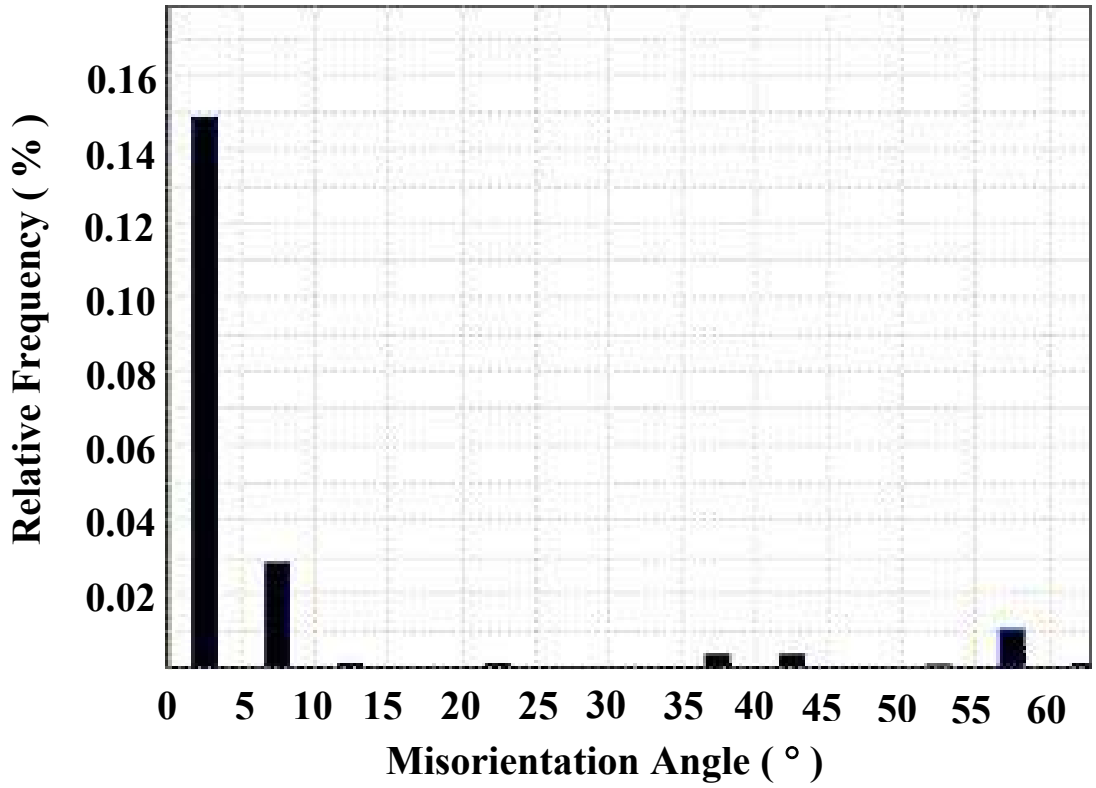

Figure 4: Misorientation angle distribution plot obtained from EBSD analysis of alloy D-9 sample hammer forged at 950°C with ~20% deformation level.

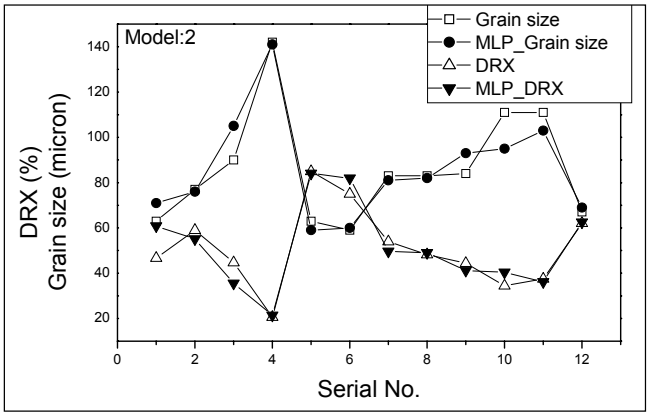

Figure 5: comparison between experimental and predicted test data in ANN Model